

# ChemComm

Accepted Manuscript



This is an *Accepted Manuscript*, which has been through the Royal Society of Chemistry peer review process and has been accepted for publication.

*Accepted Manuscripts* are published online shortly after acceptance, before technical editing, formatting and proof reading. Using this free service, authors can make their results available to the community, in citable form, before we publish the edited article. We will replace this *Accepted Manuscript* with the edited and formatted *Advance Article* as soon as it is available.

You can find more information about *Accepted Manuscripts* in the [Information for Authors](#).

Please note that technical editing may introduce minor changes to the text and/or graphics, which may alter content. The journal's standard [Terms & Conditions](#) and the [Ethical guidelines](#) still apply. In no event shall the Royal Society of Chemistry be held responsible for any errors or omissions in this *Accepted Manuscript* or any consequences arising from the use of any information it contains.

## COMMUNICATION

# Multiple CH...O Interactions involving Glycol Chains as Driving Force for the Self-Assembly of Amphiphilic Pd(II) Complexes

Cite this: DOI: 10.1039/x0xx00000x

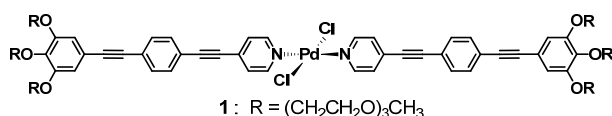
Received 00th January 2012,  
Accepted 00th January 2012Christina Rest,<sup>a</sup> Anja Martin,<sup>a</sup> Vladimir Stepanenko,<sup>a</sup> Naveen Kumar Allampally,<sup>a</sup>  
David Schmidt<sup>a</sup> and Gustavo Fernández<sup>a\*</sup>

DOI: 10.1039/x0xx00000x

www.rsc.org/

**We demonstrate that the self-assembly in polar media and gelation of an amphiphilic Pd(II) complex with pendant chlorine ligands are governed by cooperative intra- and interstrand CH...O interactions between peripheral triethylene glycol chains leading to slipped  $\pi$ -stacks.**

Self-assembled structures of amphiphilic molecules play a key role in various biological functions, such as cell compartmentalization.<sup>1</sup> Depending on external conditions as well as the size, morphology and ratio between hydrophilic and hydrophobic fragments of the monomeric units,<sup>2</sup> fascinating supramolecular structures of different dimensionality can be prepared.<sup>3</sup> The introduction of metal-containing functionalities represents a promising approach in this field,<sup>4</sup> as metal ions not only enable multiple coordination geometries with a single building block<sup>5</sup> but also provide access to catalytic, photophysical and magnetic properties.<sup>6</sup> Additionally, the resulting self-assembled structures can be further stabilized by metallophilic interactions between appropriate metal ions.<sup>7</sup> Our group has recently applied this strategy to realise fibrillar associates in nonpolar media through cooperative Pd...Pd and  $\pi$ - $\pi$  interactions by exploiting the self-assembly behaviour of an oligophenyleneethynylene (OPE)-based Pd(II) complex featuring peripheral dodecyl chains.<sup>8</sup> Motivated by these findings, we questioned whether such parallel stacks would be maintained by replacing the alkyl by polar triethyleneglycol (TEG) chains. Although amphiphilic Pt(II) complexes have received considerable attention,<sup>4</sup> their Pd(II) counterparts have been scarcely investigated.<sup>9</sup> Here, we demonstrate that the self-assembly and gelation of amphiphilic Pd(II) complexes in polar and aqueous media can be controlled by introducing peripheral TEG chains through multiple cooperative CH...O interactions.

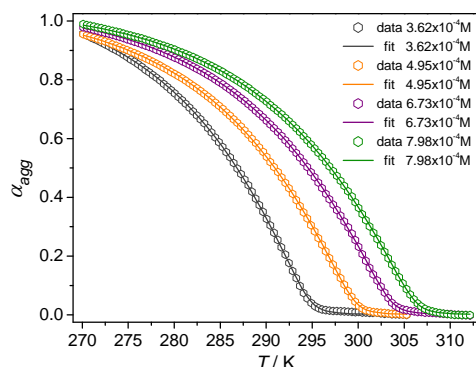


**Scheme 1.** Chemical structure of square-planar amphiphilic Pd(II) complex **1**.

To that end, we have synthesized a new Pd(II) complex **1** by reaction of OPE-based ligand **3**<sup>10</sup> with [PdCl<sub>2</sub>(PhCN)<sub>2</sub>] in 80 % yield (for characterization see SI).

**1** shows distinct spectral changes upon aggregation, as investigated by solvent-dependent UV/Vis studies (Fig. S1). In most solvents of different polarity,<sup>11</sup> the absorption maximum is located at ~346-350 nm, while in ethanol and water a bathochromic shift to 355 and 360 nm, respectively, can be noticed and a distinct shoulder around 420 nm arises (Fig. S1). The absorption at 346-350 nm can be attributed to monomeric species.<sup>8</sup> In contrast to our previously reported hydrophobic Pd(II) complex in its self-assembled state ( $\lambda_{max} = 371$  nm), the aggregate band of **1** is ~11 nm blue shifted ( $\lambda_{max} = 360$  nm) even in the poorest solvent (water) at high concentration. This behaviour suggests that the formation of parallel stacks driven by cooperative Pd...Pd and  $\pi$ - $\pi$  interactions might not be realized if the alkyl groups are replaced by bulkier glycol chains. To investigate the self-assembly process of **1**, temperature-dependent UV-Vis measurements were recorded. Water was the first solvent of choice since the solvent-dependent spectra indicated strong aggregation. However, even at 10<sup>-6</sup> M, it was not possible to monitor the whole transition to monomeric species upon heating. Alternatively, switching to less polar methanol (MeOH) enabled a complete analysis of the self-assembly mechanism. Thus, cooling curves (0.4 K/min) for solutions of **1** at four different concentrations were monitored at 425 nm (See SI), revealing a non-sigmoidal shape (Fig. 1), indicative of a cooperative supramolecular polymerization.<sup>12</sup> As shown in Figure 1, the cooperative growth does not start until the temperature falls under the critical elongation temperature  $T_e$ . At first glance, one can recognize that this temperature decreases upon decreasing concentration. To elucidate the thermodynamic parameters associated to this self-assembly process, the cooperative nucleation-elongation model developed by Ten-Eikelder, Markvoort and Meijer was successfully applied to fit the data.<sup>13</sup> For the initial thermodynamically unfavourable nucleation step, the dimerization constant  $K_2$  ranges from 0.40 to 1.14 M<sup>-1</sup>, whereas the subsequent highly favourable elongation step is characterized by a considerably larger constant  $K$  (1.3 – 2.8 x 10<sup>3</sup> M<sup>-1</sup>). This fact also becomes clear regarding the high

degree of cooperativity, described as  $\sigma = K_2/K$ , that is  $3.2 - 4.1 \times 10^{-4}$ . The enthalpy of the two distinct processes ranges from  $-20.4$  to  $-19.1$   $\text{kJmol}^{-1}$  and  $-57.2$  to  $-55.6$   $\text{kJmol}^{-1}$  for the nucleation  $\Delta H_{nucl}$  and the elongation  $\Delta H_e$ , respectively (Fig. 1, below).



Conc. [M]	$\Delta H_{nucl}^{\circ}$ [ $\text{kJmol}^{-1}$ ]	$\Delta H_e^{\circ}$ [ $\text{kJmol}^{-1}$ ]	$\Delta S^{\circ}$ [ $\text{kJmol}^{-1}\text{K}^{-1}$ ]	$T_e$ [K]	$K_2$ [ $\text{M}^{-1}$ ]	$K$ [ $\text{M}^{-1}$ ]	$\sigma$
3.62 x 10 <sup>-4</sup>	-19.1 ± 0.3	-57.2 ± 0.5	-0.1287 ± 0.0017	294.1 ± 0.05	1.14 x 10 <sup>3</sup>	2.8 x 10 <sup>3</sup>	4.1 x 10 <sup>-4</sup>
4.95 x 10 <sup>-4</sup>	-20.0 ± 0.2	-56.7 ± 0.2	-0.1262 ± 0.0007	299.1 ± 0.03	0.66 x 10 <sup>3</sup>	2.0 x 10 <sup>3</sup>	3.3 x 10 <sup>-4</sup>
6.73 x 10 <sup>-4</sup>	-20.0 ± 0.1	-55.8 ± 0.2	-0.1236 ± 0.0006	302.9 ± 0.02	0.53 x 10 <sup>3</sup>	1.5 x 10 <sup>3</sup>	3.6 x 10 <sup>-4</sup>
7.98 x 10 <sup>-4</sup>	-20.4 ± 0.1	-55.6 ± 0.2	-0.1228 ± 0.0005	305.6 ± 0.02	0.40 x 10 <sup>3</sup>	1.3 x 10 <sup>3</sup>	3.2 x 10 <sup>-4</sup>

**Figure 1.** Cooling curves obtained by monitoring the absorption of **1** in MeOH at 425 nm and fits to the ten Eikelder-Markvoort-Meijer cooperative model at four different concentrations. The table shows the corresponding thermodynamic parameters.

However, we noticed after the cooling curves were recorded that a small fraction of **1** (~15 %) partially disassembles into free ligand (**2** in SI; Fig. S2) as a result of prolonged heating and limited solubility in MeOH. Notwithstanding, considering the well-defined non-sigmoidal shape of all curves, we can hypothesize that the small fraction of free ligand has little influence on the self-assembly process of **1**.

To overcome this limitation, we tested different MeOH/dichloromethane (DCM) mixtures in order to find out whether an increase of the solubility might indeed increase the stability of the complex. We observed that **1** remained stable during the temperature-dependent measurement in MeOH/DCM (88:12) (Fig. S3), and additionally, this medium showed the best compromise in terms of solubility at high concentration and strong aggregation at low temperature. As a result of the better solvation of **1** induced by the addition of a good solvent (12 % DCM), the tendency of the system to self-assemble is significantly reduced. Thus, compared to pure MeOH a tenfold higher concentration is needed to monitor the monomer-to-aggregate transition.

Figure 2a shows the temperature-dependent UV-Vis studies of **1** (MeOH/DCM 88:12,  $3.51 \times 10^{-3}$  M) from 305 to 271 K. The maximum at 346 nm at 305 K is continuously shifting to 363 nm upon cooling, indicative of transition from monomeric to aggregated species. Similarly to MeOH, satisfactory cooling curves have been obtained at four different concentrations (Fig. 2b). The elongation temperature  $T_e$  changes significantly from 297 to 288 K upon lowering the concentration from  $3.53$  to  $1.64 \times 10^{-3}$  M. The thermodynamic parameters identified by perfect fitting to the cooperative model revealed  $\sigma$  values of

$0.6 - 2.3 \times 10^{-3}$ ,  $\Delta H_e$  values from  $-67$  to  $-56$   $\text{kJmol}^{-1}$  and nucleation ( $K_2$ ) and elongation constants ( $K$ ) of  $0.24 - 1.37$  and  $280 - 610$   $\text{M}^{-1}$ , respectively (Table S1).

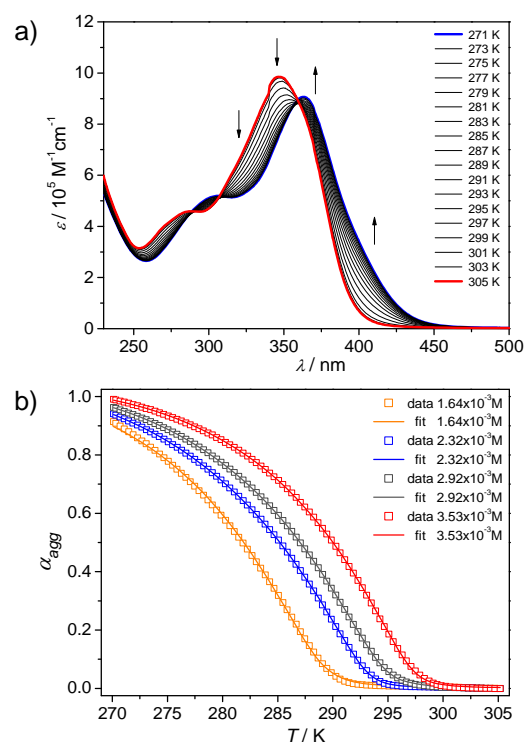


**Figure 2.** a) Temperature-dependent UV-Vis experiments of **1** (MeOH/DCM (88:12),  $3.51 \times 10^{-3}$  M). Arrows indicate the spectral changes upon decreasing temperature. b) Cooling curves obtained by monitoring the absorption of **1** in MeOH/DCM(88:12) at 425 nm.

By comparing the thermodynamic parameters in pure MeOH (Fig. 1, below) and MeOH/DCM (88:12) (Table S1), one can recognize that the addition of DCM leads to lower elongation temperatures  $T_e$  as a result of a reduced aggregation tendency. This trend also becomes noticeable regarding the binding constants. While the dimerization constant  $K_2$  shows similar values, the average elongation constant  $K$  is almost five times higher in MeOH compared to the mixture. The reliability of the model was further demonstrated by van't Hoff analysis in MeOH/DCM (88:12) (Fig. S4 and Table S2).

The cooperative self-assembly of **1** results in the instantaneous formation of stable gels in alcohols and after some weeks of aging also in water,<sup>14</sup> as investigated by atomic force microscopy (AFM), transmission (TEM) and scanning electron microscopy (SEM), in which a dense network of thin fibres can be visualized (Fig. S6-S10 and Table S3). To further investigate the structural features responsible for the cooperative process, suitable single crystals of **1** for X-Ray diffraction were grown by slow diffusion of diethyl ether into an ethanol solution of **1**. X-Ray analysis clearly reveals an almost ideal square planar configuration with diametrically arranged triethylene glycol chains (Figure S11). The packing of **1** is driven by numerous short  $\text{CH}\cdots\text{O}$  intermolecular contacts ( $<$  sum of van der Waals radii) between the TEG chains of two adjacent molecules assisted by  $\text{C-H}\cdots\text{Cl}$  interactions between the chloro ligands and two  $\text{OCH}_2$ -groups belonging to the glycol chains of every second molecule (Fig. 3, S12 and S13).

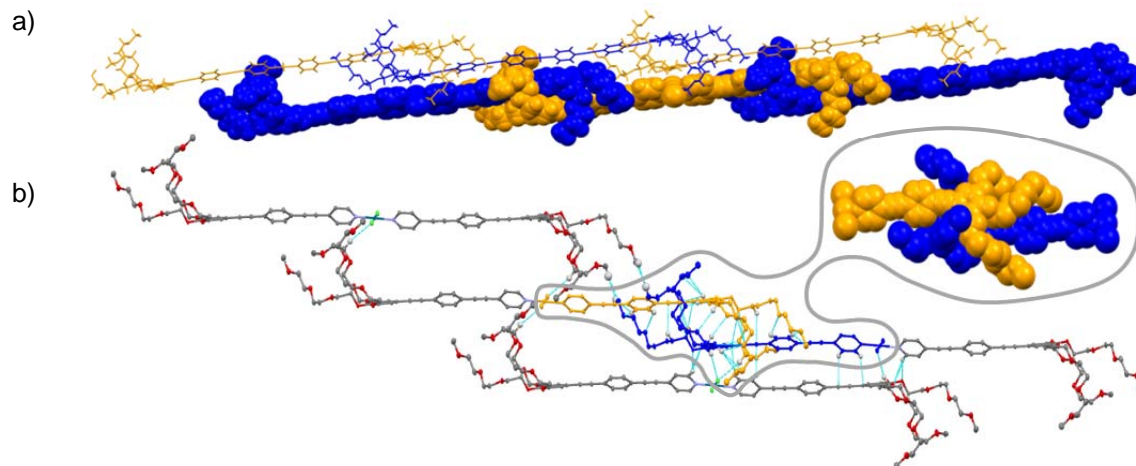


**Figure 3** a) One-dimensional double-strands of **1** arranged in a parallel fashion. b) Packing of **1** following CH...Cl contacts. Hydrogen atoms have been omitted for clarity, except those integrated in the network of weak intermolecular interactions. Atomic displacement ellipsoids are drawn at 50 % probability. Magnification of the “handshake-like” intertwining (colored in blue and orange) represented as space fill model.

Interestingly, the interplay between multiple cooperative C-H...O hydrogen bonding interactions causes the system to pack in a slipped fashion with a translationally displacement along the long axis of the molecule through CH... $\pi$  and CH...Cl interactions (Fig. 3). Such an arrangement is in perfect agreement with the packing in solution investigated by ROESY NMR (Fig. S14). The chief driving forces contributing to this arrangement are multiple C-H...O hydrogen bonding interactions between the six TEG chains of two neighboring units, which enforce an additional compact “handshake-like” intertwining that is strengthened by the incorporation of aromatic C-H bonds into the network (Figure 3b). This intertwining ultimately leads to the formation of one-dimensional double-strands that are arranged in a parallel fashion through additional interstrand contacts (Figure 3a).

In summary, we have shown that metallophilic Pd...Pd interactions cannot be realized if polar TEG chains are attached to a self-assembling Pd(II) complex with pendant chlorine ligands. Rather, the self-assembly of the amphiphilic Pd(II) complex in polar media into fibre-like structures and gels is primarily driven by cooperative inter- and intrastrand CH...O interactions between the TEG chains, also supported by aromatic and CH...Cl interactions. We expect that these weak forces can be exploited to design various metallosupramolecular amphiphilic systems in the near future.

We thank Prof. Frank Würthner for helpful discussions and the Humboldt Foundation and BMBF for financial support.

## Notes and references

<sup>a</sup> Institut für Organische Chemie and Center for Nanosystems Chemistry, Universität Würzburg Am Hubland, 97074 Würzburg (Germany).

- 1 J. H. van Esch, *Nature*, 2010, **466**, 193.
- 2 J. N. Israelachvili, *Intermolecular and Surface Forces*, Academic Press, London, **1992**.
- 3 (a) S. I. Stupp and L. C. Palmer, *Chem. Mater.*, 2014, **26**, 507; (b) A. Das, S. Ghosh, *Angew. Chem. Int. Ed.*, 2014, **53**, 2038; (c) D. Görl, X. Zhang and F. Würthner, *Angew. Chem. Int. Ed.*, 2012, **51**, 6328; (d) H.-J. Kim, T. Kim and M. Lee, *Acc. Chem. Res.* 2011, **44**, 72; (e) B. Rybtchinski, *ACS Nano*, 2011, **5**, 6791; (f) Y.-B. Lim, K.-S. Moon and M. Lee, *Chem. Soc. Rev.* 2009, **38**, 925.
- 4 (a) M. Mauro, A. Aliprandi, D. Septiadi, N. S. Kehra and L. De Cola, *Chem. Soc. Rev.*, 2014, **43**, 4144; (b) W. Li, Y. Kim, J. Li and M.

- Lee, *Soft Matter*, 2014, **10**, 5231; (c) N. Lanigan and X. Wang, *Chem. Commun.*, 2013, **49**, 8133; (d) A. Y.-Y. Tam and V. W.-W. Yam, *Chem. Soc. Rev.*, 2013, **42**, 1540; (e) K. M.-C. Wong, V. W.-W. Yam, *Acc. Chem. Res.*, 2011, **44**, 424; (f) M.-O. M. Piepenbrock, G. O. Lloyd, N. Clarke, and J. W. Steed, *Chem. Rev.*, 2010, **110**, 1960. (h) N. Kimizuka, *Adv. Polym. Sci.*, 2008, **219**, 1.
- 5 (a) M. J. Mayoral and G. Fernandez, *Chem. Sci.*, 2012, **3**, 1395; (b) G. Golubkov, H. Weissman, E. Shirman, S. G. Wolf, I. Pinkas and B. Rybtchinski, *Angew. Chem. Int. Ed.*, 2009, **48**, 926.
- 6 R. Chakrabarty, P. S. Mukherjee and P. J. Stang, *Chem. Rev.*, 2011, **111**, 6810.
- 7 (a) H. Schmidbaur, A. Schier, *Chem. Soc. Rev.*, 2012, **41**, 370; (b) S. Sculfort, P. Braunstein, *Chem. Soc. Rev.*, 2011, **40**, 2741.
- 8 M. J. Mayoral, C. Rest, J. Schellheimer, V. Stepanenko, R. Albuquerque, G. Fernández, *J. Am. Chem. Soc.*, 2013, **135**, 2148.
- 9 (a) J. Zhang, S. Chen, S. Xiang, J. Huang, L. Chen and C.-Y. Su, *Chem. Eur. J.*, 2011, **17**, 2369; (b) G. Hamasaka, T. Muto and Y. Uozumi, *Dalton Trans.*, 2011, **40**, 8859; (c) L. Yang, L. Luo, S. Zhang, X. Su, J. Lan, C.-T. Chen and J. You, *Chem. Commun.*, 2010, **46**, 3938; (d) N. Kimizuka, S. H. Lee and T. Kunitake, *Angew. Chem. Int. Ed.*, 2000, **39**, 389.
- 10 C. Rest, M. J. Mayoral, K. Fucke, J. Schellheimer, V. Stepanenko, G. Fernandez, *Angew. Chem. Int. Ed.*, 2014, **53**, 700.
- 11 Due to the limited solubility of **1** in alcohols and water, an initial thin film in DCM and THF (2 %), respectively, was formed.
- 12 (a) T. F. A. De Greef, M. M. J. Smulders, M. Wolfs, A. P. H. J. Schenning, R. P. Sijbesma, E. W. Meijer, *Chem. Rev.*, 2009, **109**, 5687; (b) C. Kulkarni, S. Balasubramanian, S. J. George, *ChemPhysChem*, 2013, **14**, 661.
- 13 (a) H. M. M. ten Eikelder, A. J. Markvoort, T. F. A. de Greef, P. A. J. Hilbers, *J. Phys. Chem. B*, 2012, **116**, 5291; (b) A. J. Markvoort, H. M. M. ten Eikelder, P. A. J. Hilbers, T. F. A. de Greef, E. W. Meijer, *Nature Commun.*, 2011, **2**, 509.
- 14 TEM studies did not reveal any observable structures prior to six weeks, whereas an aggregate transition from short (after six weeks) to longer fibers (in the gel, formed after 12 weeks) was observed (Fig. S5-6). For related examples, see: (a) A. Das, B. Maity, D. Koley and S. Ghosh, *Chem. Commun.* 2013, 5757; (b) M. R. Molla and S. Ghosh, *Chem. Eur. J.* 2012, **18**, 9860.